Journal of Oceanography, Vol. 54, pp. 437 to 442. 1998

The Sea Surface Temperature Product Algorithm of the Ocean Color and Temperature Scanner (OCTS) and Its Accuracy

FUTOKI SAKAIDA[1], MASAO MORIYAMA[2], HIROSHI MURAKAMI[3], HIROMI OAKU[3], YASUSHI MITOMI[4], AKIRA MUKAIDA[4] and HIROSHI KAWAMURA[5]

[1]*Ocean Mechanical Engineering Chair, Kobe University of Mercantile Marine, 5-1-1, Fukae-Minami-machi, Kobe 658-0022, Japan*
[2]*Computer and Information Science Department, Faculty of Engineering, Nagasaki University, 1-14 Bunkyo-machi, Nagasaki 852-8521, Japan*
[3]*Earth Observation Research Center (EORC), National Space Development Agency of Japan (NASDA), Roppongi First Building, 1-9-9, Roppongi, Minato-ku, Tokyo 106-0032, Japan*
[4]*Remote Sensing Technology Center of Japan (RESTEC), Roppongi First Building, 1-9-9, Roppongi, Minato-ku, Tokyo 106-0032, Japan*
[5]*Center for Atmospheric and Oceanic Studies, Faculty of Science, Tohoku University, Aoba, Sendai 980-8578, Japan*

(Received 29 January 1998; in revised form 7 May 1998; accepted 12 May 1998)

The Ocean Color and Temperature Scanner (OCTS) aboard the Advanced Earth Observing Satellite (ADEOS) can observe ocean color and sea surface temperature (SST) simultaneously. This paper explains the algorithm for the OCTS SST product in the NASDA OCTS mission. In the development of the latest, third version (V3) algorithm, the OCTS match-up dataset plays an important role, especially when the coefficients required in the MCSST equation are derived and the equation form is adjusted. As a result of the validation using the OCTS match-up dataset, the algorithm has improved the root mean square (rms) error of the OCTS SST up to 0.698°C although some problems remain in the match-up dataset used in the present study.

Keywords:
· OCTS/ADEOS,
· SST.

1. Introduction

The Ocean Color and Temperature Scanner (OCTS) is a passive sensor aboard the Advanced Earth Observing Satellite (ADEOS). The OCTS plans to observe ocean color and sea surface temperature (SST) simultaneously, and to that end it is equipped with eight visible (VIS) and near-infrared (NIR) bands and four thermal-infrared (TIR) bands (Table 1). The TIR bands of the OCTS can be used to calculate SST by means of the Multi-Channel SST (MCSST) technique, which is one of the methods for retrieving SST more accurately (e.g., McClain *et al*., 1985). Therefore, the OCTS can provide us with more reliable SST data.

Unfortunately, the OCTS operation terminated on June 30, 1997 due to an unexpected accident to the satellite. Consequently, the ADEOS lifetime is only about 10 months. However, huge amounts of data were obtained by the OCTS during the ADEOS lifetime. These data will contribute a great deal to our understanding the marine environment and the biological, biochemical and physical processes in the ocean due to the unique character of the OCTS, as mentioned above.

The purposes of this paper are to explain the algorithm for the OCTS SST product and to examine the algorithm and the product's accuracy. A third revision of the algorithm has been completed at the time of writing; hereafter, in this paper, this latest algorithm is called the V3 algorithm. Section 2 explains the cloud detection algorithm and the atmospheric correction algorithm in the V3 algorithm. Section 3 examines the algorithm and the accuracy of the OCTS SST product by means of a comparison between the in-situ observation data and the corresponding OCTS SST data.

2. Algorithm Description

2.1 Cloud detection algorithm

Table 2 shows the cloud detection tests used in the algorithm for the OCTS SST product. The framework of the latest cloud detection algorithm is to apply up to four tests to detect clouds and then to identify a pixel as cloud-free only when all the tests prove negative. The details of the cloud detection tests used in the V3 algorithm are given below.

The first and second tests are called a gross cloud test.

In the first test, the brightness temperature of band-11 (T_{11}) is compared with the air temperature (T_a). The T_a data are extracted from the objective analysis data provided by the Japan Meteorological Agency (JMA). A pixel is flagged as cloudy when the difference between T_{11} and T_a is greater than 20°C. In the second test, a pixel whose T_{11} is below the threshold value, –2°C, is rejected as cloud contaminated.

The third test is an NIR test in which band-8 data are used. The OCTS observation is daytime only, so that the band-8 data are always available whenever the OCTS data are obtained. In the NIR test, each band-8 value is divided by a reference value (REF). The REF is calculated using the satellite zenith angle (θ) and the sun zenith angle (θ_0) as follows:

$$\mathrm{REF} = F_0 \cdot t_{865}(\theta) \cdot t_{865}(\theta_0) \qquad (1)$$

where F_0 is the annual mean solar radiance (in units of mW·cm^{-2}·nm^{-1}) and $t_{865}(\phi)$ means the atmospheric transmittance of the 865 nm band at angle ϕ. These are calculated as follows:

$$F_0 = 8.55\{1 + 0.0167 \cdot \cos(2\pi(D - 3)/T_D)\}^2, \qquad (2)$$

$$t_{865}(\phi) = \exp\{-(0.5\tau_R + \tau_{OZ} + \tau_{OX})/\cos\phi\} \qquad (3)$$

where D is the days integrated from January 1 and T_D is total days (365 or 366 when a leap year) and τ stands for the optical thickness, $\tau_R = 0.0158$ (Rayleigh optical thickness), $\tau_{OZ} = 0.0009$ (ozone), $\tau_{OX} = 0.0$ (oxygen).

The forth test is a uniformity test. This test is known as one of the effective cloud detection tests and is widely used in many cloud detection algorithms (e.g., Saunders and Kriebel, 1988; Stowe *et al.*, 1991; Sakaida and Kawamura, 1996). In the OCTS algorithm, uniformity, which means the spatial variation in degree of reflectance or brightness temperature in a small area, is calculated as the standard deviation of a 3×3 pixel array. Added to this, uniformity is calculated not only using the band-11 brightness temperature but also using the band-8 reflectance. When the both uniformity values exceed the corresponding thresholds, the pixel is rejected as cloud contaminated. This method is called the double-uniformity method (DUM) in this paper.

The advantage of the DUM is that it is capable of avoiding errors occurring in the oceanic front region in the TIR image. Such regions often have large uniformity values due to the large temperature gradient, regardless of the cloud free condition. The DUM prevents the cloud detection error in the oceanic front region whenever the corresponding band-8 image has a large uniformity value.

Some problems remain in the V3 cloud detection algorithm. One of the problems is that a cloud detection error is apt to occur in a region affected by the sun glitter. However, the OCTS is equipped with a tilt function to

Table 1. The spectral bandwidths of the OCTS.

	Band-#	Spectral bandwidths (μm)
VIS/NIR band	1	0.392–0.432
	2	0.423–0.463
	3	0.468–0.512
	4	0.502–0.538
	5	0.545–0.585
	6	0.650–0.690
	7	0.725–0.805
	8	0.825–0.905
TIR band	9	3.550–3.880
	10	8.25–8.8
	11	10.3–11.4
	12	11.4–12.7

Table 2. Cloud detection tests and their threshold values used in the first (V1), the second (V2) and the third version (V3) algorithm.

Test name	Algorithm version		
	V1	V2	V3
Gross cloud (1)	$T_a - T_{11} > 10$ [°C]	$T_a - T_{11} > 20$ [°C]	$T_a - T_{11} > 20$ [°C]
Gross cloud (2)	—	—	$T_{11} < -2$ [°C]
NIR radiance	—	$L_8/\mathrm{REF} > 0.016$	$L_8/\mathrm{REF} > 0.0085$
TIR (1)	$T_{11} - T_{12} > 0$ [°C]	$T_{12} - T_{11} > 0.5$ [°C]	—
TIR (2)	—	$T_{10} - T_{11} > -1.5$ [°C]	—
TIR (3)	—	$T_{11} - T_{10} > 3.0$ [°C]	—
Uniformity	—	$\sigma(L_8) > 0.025$ and $\sigma(T_{11}) > 0.5$ [°C]	$\sigma(L_8) > 0.03$ and $\sigma(T_{11}) > 0.1$ [°C]

T_a: Surface air temperature from the JMA's objective analysis data.
$T_{10, 11, 12}$: Brightness temperatures of band-10, -11, and -12.
L_8: Radiance of band-8 (unit: mW·cm^{-2}·μm^{-1}).
REF: Calculated 865 nm-band radiance (see text).
$\sigma(x)$: Standard deviation on a 3×3 pixel array of parameter x.

minimize the sun-glitter effect. Therefore, it is not a serious problem if the tilt function is used.

Another problem is caused in the detection of cirrus-type cloud. In the case of the AVHRR aboard the NOAA satellite, it has been pointed out (e.g., Inoue, 1985; Ou *et al*., 1993) that cirrus-type cloud is effectively detected by the TIR test, which means a test using the brightness temperature difference in this paper. As shown in Table 2, however, the latest algorithm does not include the TIR test. The TIR tests were used in the previous versions of the algorithm (V1 and V2 in Table 2), but we noticed that the brightness temperature difference was difficult to use in the case of the OCTS. To avoid cirrus-type cloud contamination, the latest algorithm tends to use tight threshold values in almost all the tests. However, this may lead to an overestimation of the cloudy region.

2.2 Atmospheric correction algorithm

In the algorithm for the OCTS SST product, the MCSST technique is used to correct the intervening atmospheric effects in cloud-free pixels. The MCSST equation can be written in the following form:

$$\begin{aligned}\mathrm{MCSST} = {} & C_0 + C_1 \cdot T_{11} + C_2 \cdot (T_{11} - T_{12}) + C_3 \cdot (T_{11} - T_{10}) \\ & + C_4 \cdot (1/\cos\theta - 1)(T_{11} - T_{12}) \\ & + C_5 \cdot (1/\cos\theta - 1)(T_{11} - T_{10}) \end{aligned} \quad (4)$$

where θ is a satellite zenith angle and T_j is the brightness temperature (in °K) of band-j (j = 10, 11, 12). The coefficients, C_i (i = 0, 5), are assumed to be constant values, so that Eq. (4) is linear.

In the first and the second version of the algorithm, the coefficients, C_i, were derived by using the atmospheric radiative transfer model. In the V3 algorithm the coefficients are empirically determined by means of a comparison between the in-situ observation data and the OCTS data. To do this, we use the match-up dataset provided by NASDA. The details of the match-up data will be given in next section.

3. Validation of the Algorithm and SST Accuracy Using Match-Up Data

3.1 Match-up data selection

In order to examine the algorithm and the accuracy of the OCTS product, NASDA provides the match-up data, which include the collected in-situ observational data and the corresponding OCTS data extracted from the original Level 1B or Level 2 Local Area Coverage (LAC) data. The center of the extracted OCTS scene corresponds to the position of in-situ observation. The size of the scene is variable; the maximum size of the scene is 512×512 pixels.

At present (10 January, 1998), the number of the match-up data is about 300, including the data only for the ocean color product validation. Added to this, some of the match-up data are useless due to cloud contamination. We therefore selected 86 data from the match-up data to derive the MCSST coefficients in the V3 algorithm and to examine the SST accuracy; the cloud detection algorithm mentioned in Section 2 is used when the cloud-contaminated data are removed from the match-up data.

Table 3 shows the relation between the number of the selected match-up data and the time difference, which is calculated as the in-situ observation time minus the satellite observation time. Although almost all the data have a time difference of two hours or less, some data have a larger time difference. Properly speaking, the large time difference data

Table 3. The relation between the number of the selected match-up data and the time difference. The time difference is defined as that the in-situ observation time minus the satellite observation time.

Time difference (hour)	No. of data
–10~–9	1
–5~–4	1
–4~–3	1
–2~–1	43
–1~0	28
0~1	1
1~2	1
2~3	4
3~4	1
4~5	2
7~8	1
23~24	1
47~48	1
Total	86

Table 4. The coefficient sets of the MCSST equation.

Coefficient set	C0	C1	C2	C3	C4	C5
(a)	–0.4256	1.001	2.269	–0.1545	0.714	–0.05751
(b)	–44.1082479	1.163921488	3.60316327	–0.65602777	2.928163277	–0.84231541
(c)	–29.5535291	1.11186989	4.258653643	–0.64458291	1.412274883	–0.55121038
(d)	–29.7608508	1.112600304	4.243604677	–0.66372081	0.685529644	–0.37048479

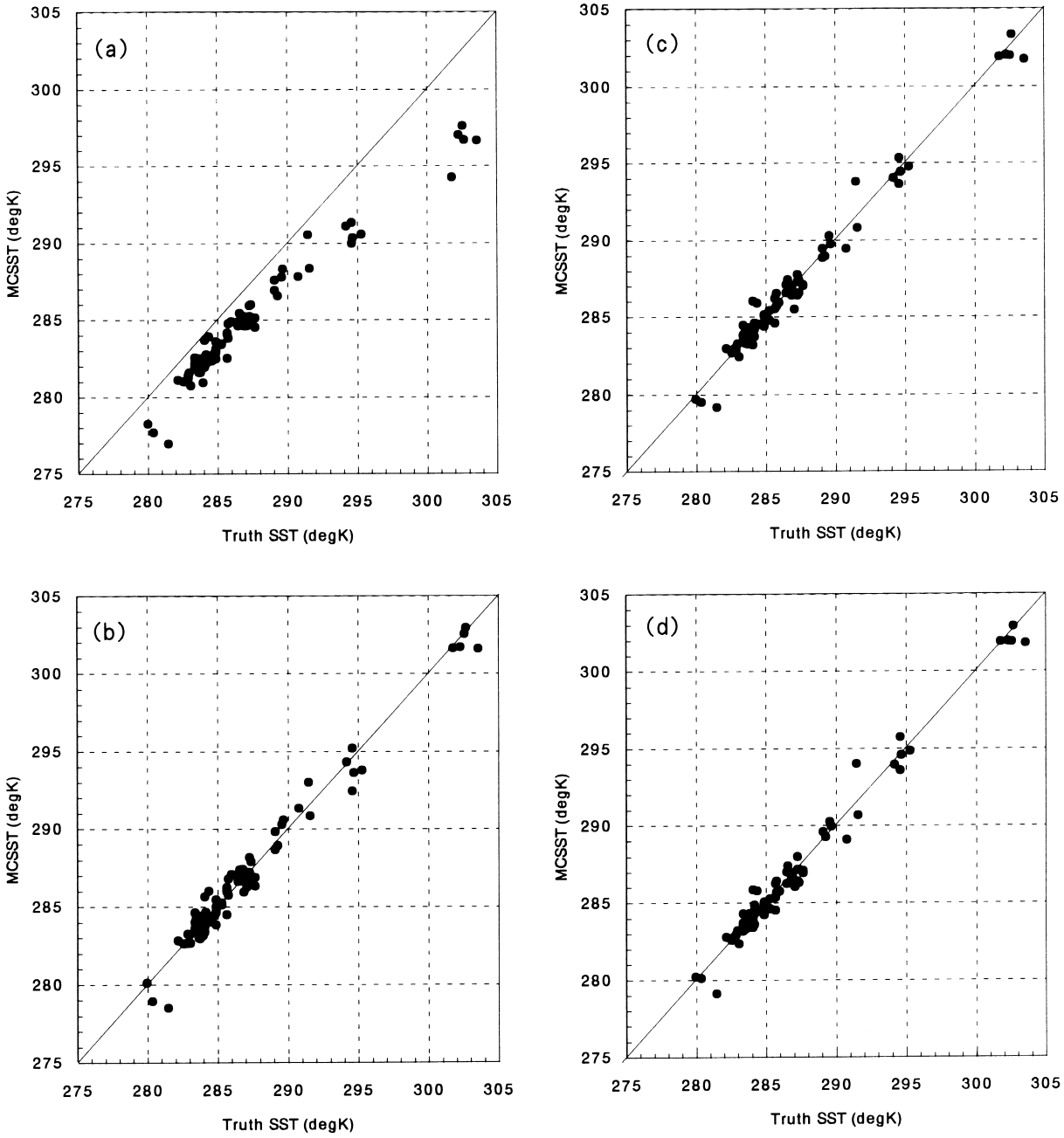

Fig. 1. The relationship between the Truth SST and the MCSST. (a) The case of the MCSST[a]. (b) The case of the MCSST[b]. (c) The case of the MCSST[c]. (d) The case of the MCSST[d].

should be omitted from the match-up data to examine the SST accuracy. However, such data are needed to increase the data whose SSTs exceed 290°K. Unfortunately, the match-up data whose SSTs exceed 290°K tend to have large time differences.

Added to this, the match-up data used in the present study include data produced by the previous (version 2) processing system of the OCTS data, because we need as many data as possible. Compared with the latest (version 3) processing system, the previous one gives less accuracy in the brightness temperature and it is possible that the large errors may occur when the geographic location is calculated (Shimada *et al*., 1998).

Consequently, some of the selected match-up data have some quality problems. Although this is unavoidable in the present study, the problems will be gradually settled as the match-up dataset increases.

3.2 Validation results

Table 4 shows the coefficient sets of Eq. (4). The coefficient set (a) in Table 4, which is used in the first and the second version algorithm, is derived by using the atmospheric radiative transfer model. In Fig. 1(a), the MCSST^a, which denotes the MCSST calculated by using the coefficient set shown in Table 4(a), is compared with the Truth SST, which means the in-situ observation data in the selected match-up data. According to Fig. 1(a), the MCSST^a is always lower than the Truth SST; this tendency becomes more noticeable as the Truth SST becomes higher. As shown in Table 5(a), the root mean square (rms) error and the bias of the MCSST^a are 2.51°K and –2.18°K, respectively.

The coefficient sets (b), (c), and (d) in Table 4 are derived by using the selected match-up data. The MCSST^b, which denotes the MCSST calculated by using Table 4(b), is compared with the Truth SST (Fig. 1(b)). The MCSST^b can correct the negative bias appearing in the case of the MCSST^a. According to Table 5(b), the rms error of the MCSST^b has improved up to 0.81°K.

According to previous studies (e.g., McClain *et al.*, 1985; McClain, 1989; Sakaida and Kawamura, 1992), the rms error is generally around 0.6°K when the MCSST technique is applied to the AVHRR data. Therefore, the rms error of the MCSST^b is still larger. One of the reasons why the rms error of the OCTS SST is larger than 0.6°K may be that the match-up data used in the present study have some quality problems.

Another reason is the contamination of the noise in the OCTS TIR band data. Figure 2(a) shows the image of the MCSST^b; the SST pattern in the image is rough due to the noise. Among the three TIR bands used in Eq. (4), the severest noise effect is found in band-12. Therefore, the average of $T_{11} - T_{12}$ is used in Eq. (4) to decrease the noise contamination. In fact, Eq. (4) can be rewritten as

Table 5. The bias and the rms error of the coefficient sets shown in Table 3. The bias is the average of MCSST-Truth SST.

Coefficient set	Bias (degK)	Rms error (degK)
(a)	–2.174	2.528
(b)	0.0	0.807
(c)	0.0	0.692
(d)	0.0	0.698

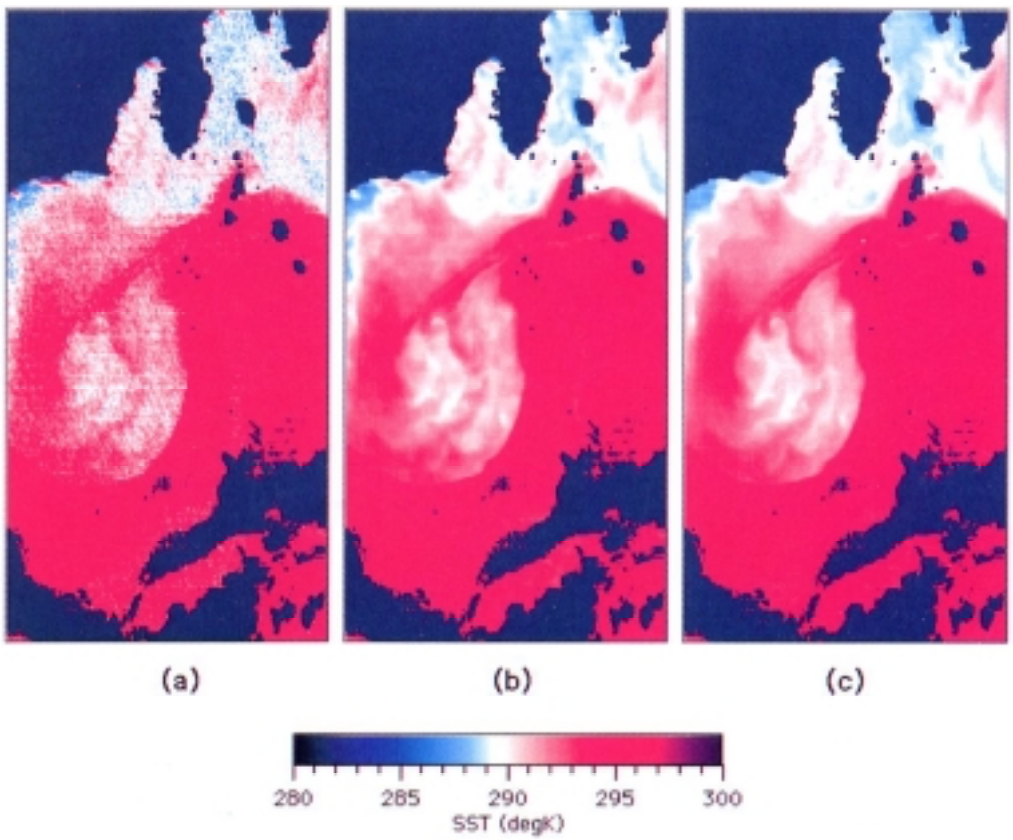

Fig. 2. The sample MCSST images at the sea area off *Enshu Nada*, Japan on April 26, 1997. (a) The case of the MCSST^b. (b) The case of the MCSST^c. (c) The case of the MCSST^d. Color code of SST is shown at the bottom of the figure.

$$\begin{aligned}\mathrm{MCSST} = {} & C_0 + C_1 \cdot T_{11} + C_2 \cdot \langle (T_{11} - T_{12}) \rangle + C_3 \cdot (T_{11} - T_{10}) \\ & + C_4 \cdot (1/\cos\theta - 1) \langle (T_{11} - T_{12}) \rangle \\ & + C_5 \cdot (1/\cos\theta - 1)(T_{11} - T_{10}) \end{aligned} \quad (5)$$

where $\langle (T_{11} - T_{12}) \rangle$ means the average of an $N \times N$ pixel array of $T_{11} - T_{12}$; N is the array size.

Table 4(c) shows the coefficient sets for the case that the array size is set at 10 ($N = 10$). The relationship between the Truth SST and the MCSST^c, which denotes the MCSST by Table 4(c), is shown in Fig. 1(c). Table 4(d) shows the coefficient sets for the case $N = 20$. Figure 1(d) shows the relationship between the Truth SST and the MCSST^d or the MCSST by Table 4(d). Figures 2(b) and 2(c) show the images of the MCSST^c and the MCSST^d, respectively. As compared with Fig. 2(a), the SST pattern appears more clearly in Figs. 2(b) and 2(c). Added to this, the rms error improves up to about 0.7°K (Table 5). Therefore, it is clear that the noise effect decreases by use of the average of $T_{11} - T_{12}$.

As for the array size, the noise effect can be suppressed more effectively when $N = 20$ than when $N = 10$, although the difference between the two is subtle. On the other hand, the rms error of the MCSST^d ($N = 20$) is 0.698°K, which is somewhat larger than that of the MCSST^c ($N = 10$), 0.692°K, according to Table 5.

4. Conclusions

To obtain the more reliable SST data from the OCTS data, the MCSST should be calculated by using the average of $T_{11} - T_{12}$. The array size, N, for averaging $T_{11} - T_{12}$ has been adopted as $N = 20$ in the V3 algorithm. Although the rms error is larger in case of $N = 20$ than in case of $N = 10$, a more clearer image can be obtained when $N = 20$. Added to this, the difference in the rms error between these two cases is small. It should be concluded, from the result of the validation using the match-up dataset, that the rms error of the OCTS SST product by the V3 algorithm is 0.698°K.

The result of the present study owes much to the existence of the match-up dataset. It is not too much to say that the operational system producing the match-up dataset was first realized in the OCTS mission in Japan. Therefore, the match-up data production can be seen as a remarkable event in the progress of satellite oceanography in Japan.

However, we note that problems still remain in the system for producing the match-up dataset. Due to this, the present study had a small match-up dataset and we were compelled to use data including poor quality items, as mentioned in Subsection 3.1. To derive more reliable parameters required in the algorithm and to improve the accuracy of the OCTS SST product, therefore, it is necessary to increase the available match-up data.

Acknowledgements

We would like to thank M. Shimada and Y. Nakamura (NASDA/EORC) for their helpful advice and supports. We also thank all the relevant institutions for providing us with the in-situ observational data in the OCTS match-up dataset. This study was supported by National Space Development Agency of Japan (NASDA) and Japan Marine Science Foundation.

References

Inoue, T. (1985): On the temperature and effective emissivity determination of semitransparent cirrus clouds by bi-spectral measurements in the 10-μm window region. *J. Meteorol. Soc. Japan*, **63**, 88–99.

McClain, E. P. (1989): Global sea surface temperatures and cloud clearing for aerosol optical depth estimates. *Int. J. Remote Sensing*, **10**, 763–769.

McClain, E. P., W. G. Pichel and C. C. Walton (1985): Comparative performance of AVHRR-based multichannel sea surface temperatures. *J. Geophys. Res.*, **90**, 11587–11601.

Ou, S. C., K. N. Liou, W. M. Gooch and Y. Takano (1993): Remote sensing of cirrus cloud parameters using advanced very-high-resolution radiometer 3.7- and 10.9-μm channels. *Appl. Opt.*, **32**, 2171–2180.

Sakaida, F. and H. Kawamura (1992): Estimation of sea surface temperatures around Japan using the Advanced Very High Resolution Radiometer (AVHRR)/NOAA-11. *J. Oceanogr.*, **48**, pp.179–192.

Sakaida, F. and H. Kawamura (1996): HIGHERS—The AVHRR-based higher spatial resolution sea surface temperature data set intended for studying the ocean south of Japan. *J. Oceanogr.*, **52**, 441–455.

Saunders, R. W. and K. T. Kriebel (1988): An improved method for detecting clear sky and cloudy radiances from AVHRR data. *Int. J. Remote Sensing*, **9**, 123–150.

Shimada, M., H. Oaku, Y. Mitomi, H. Murakami, A. Mukaida, Y. Nakamura, J. Ishizaka, H. Kawamura, T. Tanaka, M. Kishino and H. Fukushima (1998): Calibration and validation of the ocean color version-3 product from ADEOS OCTS. *J. Oceanogr.*, **54**, this volume, 401–416.

Stowe, L. L., E. P. McClain, R. Carey, P. Pellegrino, G. G. Gutman, P. Davis, C. Long and S. Hart (1991): Global distribution of cloud cover derived from NOAA/AVHRR operational satellite data. *Adv. Space Res.*, **11**, (3)51–(3)54.